Correlations between tetragonality, polarization, and ionic displacement in $PbTiO_3$-derived ferroelectric perovskite solid solutions

Tingting Qi, Ilya Grinberg, and Andrew M. Rappe
The Makineni Theoretical Laboratories, Department of Chemistry, University of Pennsylvania, Philadelphia, Pennsylvania 19104-6323, USA

(Received 7 July 2010; revised manuscript received 5 August 2010; published 15 October 2010)

We use first-principles density-functional theory calculations to investigate the dependence of tetragonality on local structure in a variety of ferroelectric solid solutions. We demonstrate that tetragonality is strongly coupled to the *B*-cation displacement and weakly coupled to the *A*-cation displacement. Examination of various $BiM^{3+}O_3$ additives to $PbTiO_3$ for different M^{3+} ionic sizes reveals that substitution of either small *B* cations or low doping of large *B* cations gives rise to large spontaneous polarization and tetragonality. Understanding how the phase transition temperature (T_c) and tetragonality are affected by Pb- and Bi-based perovskite additives provides a rational path for designing new high-temperature piezoelectric materials.

DOI: 10.1103/PhysRevB.82.134113 PACS number(s): 77.84.Lf, 71.15.Mb, 77.80.bj

Perovskite ferroelectrics are a class of materials of fundamental scientific interest as well as varied technological applications.[1–3] Tetragonal distortion of the lattice is particularly important. It has long been known that a tetragonal end member is crucial for promoting high piezoelectric performance at the solid solution's morphotropic phase boundary (MPB).[4] Recently, novel Bi-based ferroelectrics possessing extreme tetragonality ($c/a=1.1-1.25$) have been discovered,[5–8] far surpassing $PbTiO_3$ ($c/a=1.06$). The large spontaneous polarization and structural anisotropy of highly tetragonal ferroelectric materials make them promising for areas such as negative thermal expansion, multiferroics, and birefringent optics.[9–11]

A fundamental goal of materials science is to understand how a material's composition gives rise to its properties. Since the landmark paper of Devonshire,[12] Landau-Ginzburg-Devonshire (LGD) theory has been proved to be a powerful tool for studying ferroelectrics. As a phenomenological model, LGD theory treats the macroscopic observable polarization (P) as the order parameter. If the LGD parameters are known, predictions can be made relating properties to each other within a given material. However, the property changes due to compositional variation cannot be determined by standard LGD theory. The lack of an effective and quantitatively accurate theoretical tool for understanding how compositional changes affect tetragonality hinders the search for new materials with enhanced properties. Previously, we were the first to show that a simple universal proportionality relates the ferroelectric-paraelectric transition temperatures in $PbTiO_3$-based solid solutions to the square of their ground state polarization (P^2).[13,14]

In this work, using first-principles calculations, we show that the use of a microscopic property, the average cation off-center displacement, as the order parameter in the LGD framework enables prediction of tetragonality by a simple expression. The displacement-strain coupling parameter is general for a large number of $PbTiO_3$-derived ferroelectric perovskite solid solutions. We also elucidate the crystal chemical properties that control the average atomic displacement in perovskites. Together, these two advances provide a roadmap for the design of new ferroelectric materials.

We study 25 different tetragonal ferroelectric materials using density-functional theory (DFT).[15,16] The details of the computational approach are the same as in previous work.[13,14] Four different cation arrangements with minimal oxygen overbonding and underbonding[13,17] are used to study $0.25\ BiM^{3+}O_3-0.75\ PbTiO_3$. Only one cation arrangement was used for $0.125\ BiM^{3+}O_3-0.875\ PbTiO_3$. Berry's phase calculations[18] were carried out to obtain the polarization. All data are presented in Table I.

Comparison of the correlations between the experimental $c/a-1$ values and the *ab initio* data P^2, average *A*-site off-center displacement squared (D_A^2) and average *B*-site off-center displacement squared (D_B^2) shows that D_B is the parameter that controls tetragonality. Figure 1 presents a general trend of higher P corresponding to higher $c/a-1$; however, the correlation weakens at high P values. In Fig. 1, similarly poor linear correlation is found for $c/a-1$ and D_A^2. On the other hand, we find that $c/a-1$ and D_B^2 are strongly correlated, with all of the data points falling close to a straight line through the origin. Including D_A^2, D_B^2 and the D_AD_B cross terms for fitting the $c/a-1$ data does not significantly improve the correlation coefficient, proving that tetragonality is only weakly dependent on *A*-site displacement, and that the correlation between $c/a-1$ and D_A^2 comes from the coupling between the *A*- and *B*-site displacements.

It is important to note that a simple linear regression yields nonzero intercepts for $c/a-1$ vs D_A^2, and $c/a-1$ vs P^2. However, the same linear regression finds that the fit for $c/a-1$ vs D_B^2 goes naturally through the origin. The nonzero intercepts for the linear regression fits of $c/a-1$ vs D_A^2 and $c/a-1$ vs P^2 come from the large scatter in the data. If additional solid solutions were included, the values of the *x*-axis intercept for these fits should also be zero.

Our results suggest the following interpretation. First, tetragonality has a universal scaling with average *B*-cation displacement in ferroelectric $PbTiO_3$-derived solid solutions for a variety of *A*- and *B*-site compositions. Second, the modified LGD theory with *B*-site displacement replacing P as order parameter can be used to predict tetragonality of the different compositions. This model can be understood intuitively, by emphasizing that the mechanical property of tet-

TABLE I. DFT and experimental data for tetragonal $PbTiO_3$-derived ferroelectric perovskite solid solutions. A- and B-cation averaged displacements (D_A,D_B) and polarization (P), averaged over several different cation arrangements, are DFT predictions. All the displacement data listed here are for the (100) components of the total displacement vectors. Data marked by † and * are taken from our previous work, Refs. 13 and 14, respectively. The $c/a-1$ and Curie temperature (T_c) data are from experimental literature (Refs. 4 and 5). The T_c datum for $BiZn_{1/2}Ti_{1/2}O_3$ is omitted since this compound decomposed before undergoing phase transition (Ref. 6).

	$c/a-1$	P	T_c	D_B	D_A
PT†	0.065	0.87	765	0.280	0.450
0.75 $PbZn_{1/3}Nb_{2/3}O_3$–0.25 PT†	0.033	0.66	547	0.218	0.461
0.5 $PbZrO_3$–0.5 PT	0.023	0.76	659	0.165	0.440
0.5 $PbSc_{1/2}Nb_{1/2}O_3$–0.5 PT	0.020	0.50	560	0.142	0.296
0.5 $PbIn_{1/2}Nb_{1/2}O_3$–0.5 PT	0.028	0.45	623	0.129	0.255
0.375 $PbSc_{2/3}W_{1/3}O_3$–0.625 PT	0.020	0.61	517	0.176	0.350
0.375 $PbMg_{1/3}Nb_{2/3}O_3$–0.625 PT†	0.044	0.66	583	0.201	0.387
0.375 $PbZn_{1/3}Nb_{2/3}O_3$–0.625 PT†	0.048	0.74	643	0.241	0.424
0.33 $PbZrO_3$–0.67 PT	0.046	0.84	700	0.210	0.450
0.25 $PbSc_{1/2}Nb_{1/2}O_3$–0.75 PT	0.041	0.74	640	0.220	0.412
0.25 $PbIn_{1/2}Nb_{1/2}O_3$–0.75 PT	0.046	0.65	695	0.208	0.387
$BiZn_{1/2}Ti_{1/2}O_3$	0.220	1.34		0.489	0.903
0.5 $BiMg_{1/2}Ti_{1/2}O_3$–0.5 PT*	0.047	0.88	733	0.200	0.515
0.5 $BiZn_{1/2}Ti_{1/2}O_3$–0.5 PT*	0.120	1.17	1100	0.365	0.675
0.25 $BiMg_{1/2}Zr_{1/2}O_3$–0.75 PT*	0.041	0.86	721	0.216	0.478
0.25 $BiMg_{1/2}Ti_{1/2}O_3$–0.75 PT*	0.061	0.93	803	0.258	0.505
0.25 $BiZn_{1/2}Zr_{1/2}O_3$–0.75 PT*	0.064	0.93	740	0.263	0.508
0.25 $BiZn_{1/2}Ti_{1/2}O_3$–0.75 PT*	0.088	1.04	875	0.319	0.550
0.25 $BiScO_3$–0.75 PT	0.040	0.84	768	0.220	0.488
0.25 $BiGaO_3$–0.75 PT	0.057	0.84	768	0.226	0.447
0.25 $BiInO_3$–0.75 PT	0.080	0.90	856	0.257	0.539
0.125 $BiAlO_3$–0.875 PT	0.050	0.84	758	0.243	0.473
0.125 $BiScO_3$–0.875 PT	0.053	0.85	780	0.257	0.442
0.125 $BiGaO_3$–0.875 PT	0.057	0.83	757	0.241	0.427
0.125 $BiInO_3$–0.875 PT	0.077	0.94	847	0.295	0.535

ragonality should be more strongly correlated with another mechanical property, atomic displacement, rather than an electrical property such as polarization. We describe the strain-displacement coupling contribution to the free energy in terms of D_A and D_B by

$$G = -\gamma_A s D_A^2 - \gamma_B s D_B^2 - \gamma_{AB} s D_A D_B + \frac{1}{2} K s^2, \qquad (1)$$

where strain s is the tetragonality $c/a-1$, and γ and K are the strain-displacement coupling and the elastic constants, respectively. Minimizing the free energy with respect to s, we get

$$s = (\gamma_A D_A^2 + \gamma_B D_B^2 + \gamma_{AB} D_A D_B)/K. \qquad (2)$$

The high quality of the fit to D_B^2 data in Fig. 1 means that γ_A and γ_{AB} are small compared to γ_B, and can be neglected.

On the other hand, if the free energy G is written in a standard form with the overall polarization P_{tot} as the order parameter, the minimum-energy s is given by

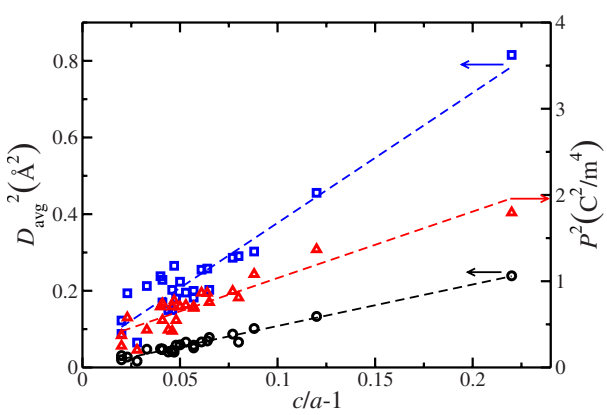

FIG. 1. (Color online) Linear correlations for the average cation displacement (D_A^2 in blue squares and D_B^2 in black circles) vs experimentally observed $c/a-1$ and theoretical P^2 vs experimentally observed $c/a-1$ (P^2 in red triangles) are shown. Unlike D_A^2 and P^2, D_B^2 is closely correlated with $c/a-1$. All of the fits shown are forced to cross the origin.

TABLE II. Fitting functions set I (simple linear regression) and set II (forced to cross the x axis at the origin). R is the notation for correlation coefficient. By using different fitting variables to fit strain (s), we conclude that D_B^2 is the most universal parameter with the best linear correlation with s. Fitting parameters a, b, and d are in the unit of $Å^{-2}$, e is in the unit of $m^4\ C^{-2}$, and c is unitless.

Fitting functions set I	R
aD_A^2+c	0.958
$a=0.2703$, $c=-0.0054$	
bD_B^2+c	0.984
$b=0.8938$, $c=0.0020$	
$aD_A^2+bD_B^2+c$	0.985
$a=0.0553$, $b=0.7236$, $c=-0.0003$	
dD_AD_B+c	0.983
$d=0.5016$, $c=-0.0025$	
$aD_A^2+bD_B^2+dD_AD_B+c$	0.986
$a=-0.2646$, $b=-0.5987$, $d=1.2928$, $c=0.002$	
eP^2+c	0.924
$e=0.1108$, $c=-0.0208$	

Fitting functions set II	R
aD_A^2	0.946
$a=0.2466$	
bD_B^2	0.984
$b=0.9058$	
$aD_A^2+bD_B^2$	0.985
$a=0.0530$, $b=0.7201$	
dD_AD_B	0.981
$d=0.4820$	
$aD_A^2+bD_B^2+dD_AD_B$	0.986
$a=-0.2664$, $b=-0.6019$, $d=1.3082$	
eP^2	0.807
$e=0.0816$	

$$s = \gamma(Z_A^* D_A + Z_B^* D_B)^2/K, \tag{3}$$

where we express P_{tot} as the sum of the A- and B-site contributions given by the average product of cation displacement and its Born effective charge Z^*. This forces the coupling constants between s and A- and B-site off-center displacements squared to scale as their respective Z^* squared. In Table II set I, fit $aD_A^2+bD_B^2+c$ shows that the γ_B/γ_A ratio is ≈ 13, much larger than the $(Z_B^*/Z_A^*)^2=3.4$ ratio for $PbTiO_3$. The disagreement is even worse for $BiZn_{1/2}Ti_{1/2}O_3$, where $(Z_B^*/Z_A^*)^2=1.4$. The overestimation of the A-site contribution in the fit of s data to P^2 weakens the correlation and leads to the unphysical result that $P_{tot}\neq 0$ when $s=0$, fit eP^2+c in Table II set I, making P_{tot} a less accurate predictor of c/a.

The interplay between bonding and geometry in a perovskite structure explains the differences in the strain dependence on the cation displacements of the A and B sites. We consider a strain along the (100) direction. For the B cations, a (100) off-center displacement is along the O-B-O axis and strongly affects the B-O bond orders along that direction. Increased strain elongates the (100) lattice constant allowing more space for the B-cation distortion and making B-cation off-centering displacement more favorable.[19] For the A site, there is a $\approx 45°$ angle between the (100) direction of the A-cation off-center displacements and the (110) direction of the A-O bonds. In this case, a tetragonal strain leads to relatively small changes in the A-O bond length and its bond order. Hence, displacement-strain coupling for the A cations is not as strong as for the B cations.

At first glance, the weak correlation between $c/a-1$ and P found in our work contradicts the well-known scaling of the tetragonality with the square of polarization as temperature is varied. However, since D_A and D_B are coupled for a single material, temperature variation changes P_A and P_B, and therefore P_{tot} in a similar way, so that P_{tot} has a strong correlation with $c/a-1$ as T is varied. However, changing the composition affects one cation site more strongly than the other. For example, P_A is more affected by A-site substitution while P_B is more affected by the B-site substitution. As a result, the correlation between $c/a-1$ and P_{tot}^2 is much weaker for compositional variation.

The relationship between D_B and c/a elucidated here, as well as the previously obtained correlation between P and T_c reduce the problem of new ferroelectric material design to that of enhancing D_A and D_B values. In previous work, we found that DFT-obtained cation displacements D_M in ferroelectric $PbTiO_3$-based solid solutions are remarkably transferable from one material to another.[14] The displacement tendency of each cation can therefore be characterized by parameter D_M^0, the displacement that cation M would make in almost pure $PbTiO_3$ at a very low doping fraction. The D_M^0 value variation cannot be explained by ionic size argument alone, since it is also closely related to the covalency of the M-O bond, with higher covalency leading to enhanced ionic displacement. This can be illustrated by a comparison of the more covalent Zn^{2+} ($D_{Zn}^0=0.25$ Å, $R_{Zn}=0.74$ Å) and more ionic Mg^{2+} ($D_{Mg}^0=0.08$ Å, $R_{Mg}=0.72$ Å) cations.[13,14]

Here, we examine the ionic size R impact on D_B, by holding D_B^0 nearly constant. We performed *ab initio* calculations on x $BiMO_3-(1-x)$ $PbTiO_3$ ($M^{3+}=Al^{3+}$, Ga^{3+}, Sc^{3+}, and In^{3+}) (Ref. 20). Figure 2 shows that both $D_{A,avg}$ and $D_{B,avg}$ average displacement magnitudes depend nonmonotonically on the average B-cation ionic size $R_{B,avg}$, implying two competing effects exist, and they switch dominant role depending on $R_{B,avg}$. Figure 2 also shows that the two effects are influenced by the doping fraction of $BiMO_3$. The B-site displacements are more sensitive to the change in x, as seen by a larger shift of the minimum cation displacement values. Next, we discuss the two effects for small and large ionic size substituents.

When R_M is small, the increase in the ionic displacement for smaller B site can be explained by the well-known rattling cation effect. The mismatch between the short cation-oxygen bonds preferred by the dopant ion and the larger lattice constant preferred by the A-O sublattice favors off-centering of the dopant and an increase in the average A-site and B-site displacements.

When R_M is large, the increased ionic displacements D_B for large substituent B-site ions (e.g., In^{3+}) are due to the

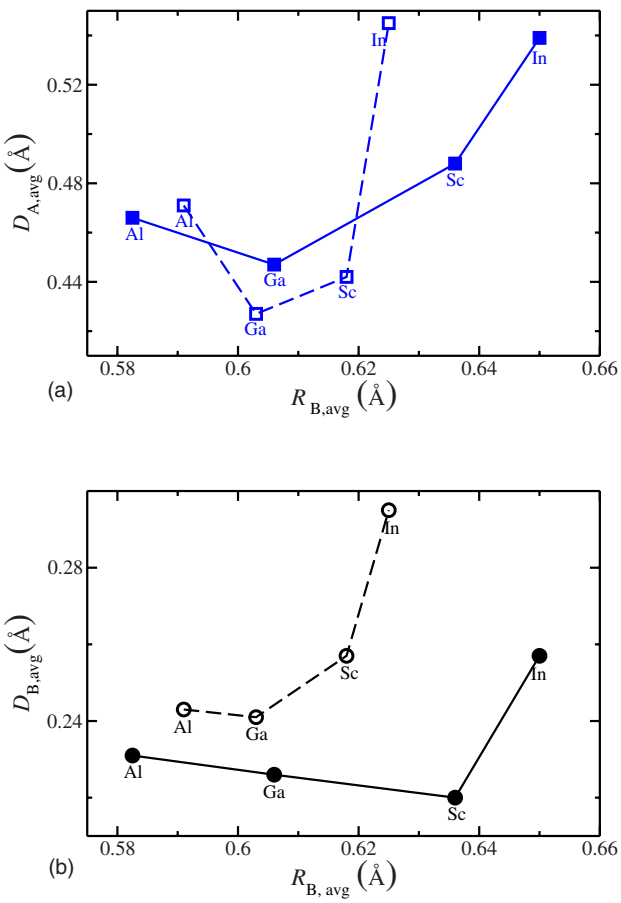

FIG. 2. (Color online) The average B-cation ionic size effect $R_{B,\mathrm{avg}}$ on average cation displacement D_A (a) blue squares) and D_B (b) black circles) in solid solution x $\mathrm{Bi}M^{3+}\mathrm{O}_3-(1-x)$ PbTiO_3 is shown. Compositions $x=0.125$ and $x=0.25$ are noted as unfilled and filled symbols, respectively. Ionic displacements are increased by substitution of either very large (In^{3+}, $R_{\mathrm{In}}=0.80$ Å) or very small (Al^{3+}, $R_{\mathrm{Al}}=0.53$ Å) R_M.

expansion of the crystal volume. Introducing very large cations on the B-site creates a conflict between the preference of the substituent for a larger unit cell volume and the preference of the A cations for a smaller A-O sublattice. Usually, such a conflict is resolved by the rotation of the B-O_6 octahedra; however, for a low concentration of large B cations, the stiffness of the TiO_6 octahedra in PbTiO_3 and their resistance to tilting make these large rotations energetically unfavorable.[21] Instead, the A-site off-centering increases, bringing the A cations closer to the O anions to achieve the desired short A-O bonds. Thus, in a solid solution, alloying a larger volume perovskite into a smaller volume one expands the A site for the smaller A cations, equivalent to applying negative pressure[22] to the smaller volume perovskite.

The understanding of the relationships between cation characteristics and the technologically important T_c and c/a properties of perovskite ferroelectrics provides guidance for the design of new materials with enhanced performance. For example, the finding that tetragonality scales with the B-site displacement means that compositions with a small charge on the A site (e.g., Ag^+-based ABO_3) can be extremely tetragonal. For enhancement of c/a and P at small dopant fraction, large cation size and displacement are favorable. At higher substituent fraction, smaller ionic size is favorable, suggesting that cations such as Al^{3+} ($R_{\mathrm{Al}}=0.53$ Å) and V^{4+} ($R_{\mathrm{V}}=0.58$ Å) and V^{5+} ($R_{\mathrm{V}}=0.54$ Å) are promising for enhancing polarization and c/a.

For PbTiO_3-derived piezoelectric materials, the highest performance occurs at the MPB. For operation at high temperatures, the T_c at the MPB must be high. To create an MPB, a rhombohedral or antiferroelectric perovskite is mixed with PbTiO_3, to destabilize the tetragonal phase and reduce c/a (typically, MPB compositions exhibit $c/a \approx 1.025$). From the demonstrated correlations above, reduction in c/a means that the B-site displacement must be diminished. However, high T_c is favored by large polarization, with contributions from both A- and B-cation displacements. Hence, the optimal strategy is to mix in a perovskite with $D_B^0 < D_{\mathrm{Ti}}^0$ and $D_A^0 > D_{\mathrm{Pb}}^0$; this decreases c/a while the increased A-site polarization compensates for the smaller B-site P contribution. Another strategy is to substitute large cations on the B site. As shown above (Fig. 2) at higher x, a large substituent increases D_A while decreasing D_B, driving c/a down while maintaining a high P and T_c. This type of combination is in fact observed for the x $\mathrm{BiScO}_3-(1-x)$ PbTiO_3 (Ref. 23) and x $\mathrm{BiMg}_{1/2}\mathrm{Ti}_{1/2}\mathrm{O}_3-(1-x)$ PbTiO_3 (Refs. 4 and 24) solid solutions. These exhibit an immediate decrease in c/a but an initial rise in T_c which leads to enhanced T_c^{MPB} compared to the classic $\mathrm{Pb(Zr,Ti)O}_3$.

In conclusion, using DFT calculations we have revealed a universal scaling of c/a in ferroelectric perovskites with the displacement of the cation B site. The developed composition-structure-property relations provide guidance for systematic exploration of new materials.

We thank P. K. Davies for discussions about crystal chemistry. T.Q. and I.G. were supported by the Office of Naval Research under Grant No. N00014-09-1-0157. A.M.R. was supported by the Department of Energy under Grant No. DE-FG02-07ER46431. Computational support was provided by the Center for Piezoelectrics by Design, and the HPCMO of the DoD.

[1] L. Bellaiche, A. Garcia, and D. Vanderbilt, Phys. Rev. Lett. **84**, 5427 (2000).
[2] Y. Saito, H. Takao, T. Tani, T. Nonoyama, K. Takatori, T. Homma, T. Nagaya, and M. Nakamura, Nature (London) **432**, 84 (2004).
[3] D. I. Bilc and D. J. Singh, Phys. Rev. Lett. **96**, 147602 (2006).
[4] M. R. Suchomel and P. K. Davies, J. Appl. Phys. **96**, 4405 (2004).
[5] M. R. Suchomel and P. K. Davies, Appl. Phys. Lett. **86**, 262905 (2005).

[6] M. R. Suchomel, A. M. Fogg, M. Allix, H. Niu, J. B. Claridge, and M. J. Rosseinsky, Chem. Mater. **18**, 4987 (2006).
[7] D. M. Stein, M. R. Suchomel, and P. K. Davies, Appl. Phys. Lett. **89**, 132907 (2006).
[8] I. Grinberg, M. R. Suchomel, W. Dmowski, S. E. Mason, H. Wu, P. K. Davies, and A. M. Rappe, Phys. Rev. Lett. **98**, 107601 (2007).
[9] J. Chen, X. Xing, C. Sun, P. Hu, R. Yu, X. Wang, and L. Li, J. Am. Chem. Soc. **130**, 1144 (2008).
[10] P. Hu, J. Chen, J. Deng, and X. Xing, J. Am. Chem. Soc. **132**, 1925 (2010).
[11] S. Ju and G. Y. Guo, J. Chem. Phys. **129**, 194704 (2008).
[12] A. F. Devonshire, Philos. Mag. **40**, 1040 (1949).
[13] I. Grinberg and A. M. Rappe, Phys. Rev. B **70**, 220101 (2004).
[14] I. Grinberg and A. M. Rappe, Phys. Rev. Lett. **98**, 037603 (2007).
[15] P. Hohenberg and W. Kohn, Phys. Rev. **136**, B864 (1964).
[16] J. P. Perdew and A. Zunger, Phys. Rev. B **23**, 5048 (1981).
[17] I. Grinberg, V. R. Cooper, and A. M. Rappe, Phys. Rev. B **69**, 144118 (2004).
[18] D. Vanderbilt and R. D. King-Smith, Phys. Rev. B **48**, 4442 (1993).
[19] R. E. Cohen, Nature (London) **358**, 136 (1992).
[20] 0.25 $BiAlO_3$−0.75 PT lattice constants are estimated from extrapolation.
[21] S. V. Halilov, M. Fornari, and D. J. Singh, Appl. Phys. Lett. **81**, 3443 (2002).
[22] S. Tinte, K. M. Rabe, and D. Vanderbilt, Phys. Rev. B **68**, 144105 (2003).
[23] R. E. Eitel, S. J. Zhang, T. R. Shrout, C. A. Randall, and I. Levin, J. Appl. Phys. **96**, 2828 (2004).
[24] C. A. Randall, R. Eitel, B. Jones, T. R. Shrout, D. I. Woodward, and I. M. Reaney, J. Appl. Phys. **95**, 3633 (2004).